Project	SEAMLESS No 101004032	**Start / Duration**	1 January 2021/ 36 Months
Dissemination	Public	**Nature**	Report
Date	25/05/2022	**Version**	1.0

Deliverable 3.2

Observability of the target indicators and parameter sensitivity in the 1D CMEMS sites

Deliverable Contributors:	Name	Organisation	Role / Title
Deliverable Leader	Stefano Ciavatta	PML	Task leader/project coordinator
Contributing Author(s)	Paolo Lazzari	OGS	Co-I
	Eva Álvarez	OGS	Co-I
	Jorn Bruggeman	BB	Co-I
	Arthur Capet	UGA	Co-I
	Gianpiero Cossarini	OGS	Co-I
	Farshid Daryabor	AWI	Co-I
	Lars Nerger	AWI	Co-I
	Jozef Skakala	PML	Co-I
	Anna Teruzzi	OGS	Co-I
	Tsuyoshi Wakamatsu	NERSC	Co-I
	Çağlar Yumruktepe	NERSC	Co-I
Reviewer(s)	Pierre Brasseur	UGA	Co-I
Final review and approval			

Project	SEAMLESS No 101004032	**Start / Duration**	1 January 2021/ 36 Months
Dissemination	Public	**Nature**	Report
Date	25/05/2022	**Version**	1.0

Document History:

Release	Date	Reason for Change	Status	Distribution
1.0		Initial document, reviewed	Released	Public

To cite this document

Ciavatta, S., Lazzari, P., Alvarez, E., Bruggeman, J., Capet, A., Cossarini, G., Daryabor, F., Nerger, L., Skakala, J., Teruzzi, A., Wakamatsu, T., Yumruktepe, C. (2022). D3.2 Observability of the target indicators and parameter sensitivity in the 1D CMEMS sites. Deliverable report of project H2020 SEAMLESS (grant 101004032), doi: 10.5281/zenodo.6580236

TABLE OF CONTENTS

1. Scope

This Report presents the developments, results and recommendations of Task 3.2 of WP3: " Screening of the observability and controllability of the target indicators". This task was led by PML and carried out by all the project partners, in a strict and effective collaboration between months 8 and 13 of the project. A significant part of the work was developed during a two-day hands-on workshop in Trieste (8-10 October 2021) hosted by OGS. This event was key in facilitating the definition of the analysis protocols common to all models used by the partners, ensuring the comparability of their results. This comparability was further enhanced by performing the analysis on the same high-performance-computer, kindly provided by the Italian CINECA.

In the SEAMLESS Grant Agreement, Task WP3.2 is subdivided in two subtasks:

Task 3.2a Observability and controllability analysis, which aims at identifying what ecosystem indicators can be estimated by assimilating biogeochemical variables in the CMEMS models. This objective was achieved through a sensitivity analysis of the simulated indicators with respect the observable variables.

Task 3.2b Parameters for ensemble generation, which aims at identifying what model parameters should be perturbed to represent the uncertainty of the ecosystem indicators in ensemble assimilative simulations. This objective was achieved through a sensitivity analysis of the simulated indicators with respect to the model parameters.

This report presents the work of Task 3.2 in three mains sections. Firstly, we summarized the methods that are common to the two sub-tasks 3.2a and 3.2b. Then, the motivation, approach and outcomes of the two tasks are presented and discussed in two separate sections.

2. Methods

2.1 The models

The sensitivity analyses were performed by using five biogeochemical models run operationally in the Monitoring and Forecasting Centers (MFCs) of the Copernicus Marine Service, here used in one-dimensional configurations. These models differ for their level of complexity, which is here defined using the number of plankton functional types (PFTs) in the model equations, for simplicity: "high-complexity" models have 4 PFTs or more, otherwise they have an intermediate complexity. The complexity is expected to have implications on which ecosystem indicators are observable and controllable when using the different models.

The intermediate complexity models are:

The **PISCES** model (Aumont et al. 2015) is a semi-complex carbon-based model that simulates marine biological productivity and carbon biomass based upon 5 main nutrients: nitrate, ammonium,

phosphate, silicate and iron. Its architecture includes 24 BGC variables grouped into four main compartments: nutrients, phytoplankton, zooplankton, and detritus. The phytoplankton compartment (PHY) is represented by two different classes, the nanophytoplankton and the diatoms, while the zooplankton compartment contain two species, meso- and microzooplankton. the detritus compartment is divided in 2 pools: the dissolved organic carbon (DOC) and the particulate organic matters including the small particles and the big particles which mostly differ by their sinking velocity. PISCES has been used in global simulations (e.g., Bopp et al., 2015), environmental studies (e.g., Brasseur et al., 2009), climate studies (Lefort et al., 2015), in regional scale studies (e.g., Sotillo et al., 2015) and analysed in parameter sensitivity analyses (e.g., Garnier et al., 2016). PISCES is used in the CMEMS global (GLO) and Iberian-Biscay-Irish (IBI) MFCs and it is applied in an Atlantic configuration in SEAMLESS.

The **ECOSMO** model (Daewel and Schrum, 2013) is an intermediate complexity model with four nutrients (nitrate, ammonium, phosphate and silicate) and three phytoplankton groups (flagellates, diatoms and nitrogen fixing cyanobacteria). Chlorophyll is included as a prognostic variable following Bagniewski et al. (2011). Zooplankton are represented by two size classes (micro and meso). In addition the model includes particulate and dissolved organic matter and oxygen. A simple representation of the sediment layer including sedimentation, resuspension, remineralization and denitrification under low oxygen conditions is included in the model. The model currency is carbon and a fixed Redfield ratio is applied to the other elements. ECOSMO was originally developed for the North and Baltic Sea, but was coupled to the ocean model HYCOM and adapted to the North Atlantic and Arctic. ECOSMO is used in the Arctic (ARC) MFC real time operational BGC model since April 2017.

The **ERGOM** model (Neumann, 2000) is an intermediate complex nitrogen-based model that was originally developed for the Baltic Sea and later extended for the North Sea (Maar et al., 2011). ERGOM simulates the BGC cycling in the coastal seas using three phytoplankton groups (cyanobacteria, flagellates, diatoms), two zooplankton size groups, four nutrient groups (nitrate, ammonium, phosphate, and silicate), two detritus groups (N-Detritus and Si-Detritus), oxygen and labile dissolved organic nitrogen in the water column. Further a carbonate system is included to compute partial pressure of CO_2 (pCO2) and the pH value. In our configuration, chlorophyll-a concentration is not light-dependent and is computed diagnostically. ERGOM is used in the Baltic MFC. ERGOM has been used in different studies, e.g. to study inflows to the Gulf of Finland (Lessin et al., 2014) and to assess strongly-coupled data assimilation (Goodliff et al., 2019).

The high-complexity models are **ERSEM** (Baretta et al.; 1995, Butenschön et al., 2016) in North West shelf -seas MFC) and **BFM** (Vichi et al., 2007 and Vichi et al., 2015) have several features in common, both in the structures and outputs, making it convenient to list their difference rather than describing them separately, here and in the section of the results, respectively. They both distinguish between five chemical components: carbon, chlorophyll, nitrogen, phosphorus and silicon, using variable stoichiometry for the simulated plankton groups (e.g., Geider et al., 1997; Baretta et al., 1995). The models split phytoplankton into four functional types largely based on their size (e.g., Baretta et al., 1995): picophytoplankton, nanophytoplankton, diatoms and dinoflagellates. Each Phytoplankton Functional Type (PFT) biomass is represented in terms of chlorophyll, carbon, nitrogen and

phosphorous, with diatoms also represented by silicon. Model predators are composed of three (ERSEM), or four (BFM) zooplankton types, with organic material being decomposed by one functional type of heterotrophic bacteria. The model inorganic component consists of nutrients (nitrate, phosphate, silicate, ammonium and carbon) and dissolved oxygen. The carbonate system is also included in both ERSEM (Artioli et al., 2012) and BFM (Cossarini et al., 2015; Canu et al., 2015) models. The ERSEM configuration used in SEAMLESS is the one of Butenschön et al. (2016), with the addition of a bio-optical module (Skákala et al., a, 2020), capable of resolving underwater light both spectrally and directionally. The BFM configuration is the one described in Salon et al. (2019), Lazzari et al. (2012, 2016). ERSEM and BFM are used in the CMEMS North-West Shelf-Seas (NWS) and Mediterranean (MED) MFCs, respectively.

2.2 The marine ecosystem indicators

The ecosystem indicators targeted by this project have been selected taking account of: (1) United Nations Sustainable Development Goals (UN SDGs); (2) The Global Ocean Observing System Essential Ocean and Biodiversity Variables (EOVs and EBVs); (3) CMEMS Ocean Monitoring Indicators (OMIs) and CMEMS user needs. Additional technical criteria for the selection of the indicators are: i) the capability to simulate them reliably with the state-of-the-art biogeochemical models run by modern operational centres; ii) the potential capability to constrain the simulation of these indicators by using the current operational monitoring infrastructures. Assessing such potential capability is the ultimate objective of this work.

The list of the SEAMLESS indicators includes:

A) Particulate Organic Carbon
B) Trophic efficiency
C) Primary production
D) pH
E) Dissolved oxygen
F) Phytoplankton functional types
G) Phytoplankton phenology

In the following paragraphs, a brief description of each indicator is given along with its computational definition adapted to the different SEAMLESS model formulations.

A) the **Particulate Organic Carbon (POC)** is defined here as the non-living carbon fraction of particulate organic matter, i.e. the detritus, and is computed as the average concentration of the 0-200m layer from the model output, or 0-bottom in shallower areas. Three models (BFM, ERGOM and ECOSMO) have one state variable for the particulate detritus, ERSEM and PISCES have two state variables that are summed. The unit is mmolC m^{-3}.

B) the **trophic efficiency** is the ratio of production at one trophic level to production at the next lower trophic level. It can be calculated by the percentage of energy that consumers in one trophic level gain and convert into biomass from the total stored energy of the previous trophic level. (Eddy et a., 2021). Alternatively, as commonly done in food web and ecosystem modelling, the ratio between the

biomass of upper and lower trophic levels can be used as a proxy measure of the trophic transfer efficiency within the food web (Armengol et al., 2019; Eddy et al., 2021). Considering that SEAMLESS target the link between primary producers and high trophic level components, the trophic efficiency indicator is defined as the ratio between biomass of zooplankton and phytoplankton. Given the fact that different model has a different complexity in describing the food web (i.e., number of functional groups describing primary producers, consumers and predators), the definitions of primary producer trophic level and of predator trophic level depends on the specific model as shown in the Table 1.1:

Table 2.1 Definition of trophic efficiency (i.e. the ratio of biomass of consumer trophic level and biomass of primary producer trophic level) in the SEAMLESS models, which are characterized by different numbers and types of phytoplankton groups

Model	primary producer trophic level	consumer trophic level	note
PISCES	Sum of all 2 phyto o groups	Sum of all 2 zoo groups	
ECOSMO	Sum of all 3 phyto groups	Sum of all 2 zoo groups plus detritus	
ERGOM	Sum of all 3 phyto groups	Sum of all 2 zoo groups	Nitrogen biomasses are converted into carbon using Redfield ratio
BFM	sum of 3 out of 4 phyto groups	sum of all 4 zoo groups	Heterotrophic Nano Flagellates group is excluded because it channels energy mostly in microbial food web (bacterial) and it is preyed by other zoopl. groups
ERSEM	sum of all 4 phyto groups	sum of all 3 zoo groups	

Biomasses of primary producer and consumer are computed as the vertical integral of the concentrations of the state variables in the 0-200m layer in deep ocean waters. Trophic efficiency has not unit (i.e., biomass over biomass).

C) the **primary production** is the synthesis of organic compounds from dissolved carbon dioxide through photosynthesis as source of energy. Models compute primary production as the difference between gross primary production (photosynthesis) and the internal phytoplankton respiration according to their specific formulations. Primary production is computed as the vertical integral of the 0-200m layer. The unit is mmolC m^{-2} d^{-1}.

D) the **pH** is a measure of the ocean acidity. All CMEMS models feature a carbonate system formulation that provides the pH as a diagnostic variable in total scale and at the *in situ* condition. The pH is computed as the vertical average of the 0-200m layer from the model output. pH has no unit.

E) the **dissolved oxygen** is a state variable in all CMEMS models. The oxygen indicator refers to the concentration of oxygen at the depth of 150m (model output is averaged in the layer 145-155m) or at the bottom of the water column for shallow water areas. The unit is mmolO2 m-3.

F) the **Phytoplankton Functional Types** (PFT) indicator is defined as the ratio between large phytoplankton biomass and total phytoplankton biomass. It measures the dominance of the large phytoplankton groups over the whole phytoplankton community. Large phytoplankton sustains the herbivorous food chain (large phyto-mesozoo-fishes) while small phytoplankton is comparatively more relevant to the microbial food web (Cushing, 1989; Legendre and Rassoulzadegan, 1995). Our PFT ratio indicators provides an indication of the relative importance of the two pathways. Given the different formulations of the SEAMLESS/CMEMS models, the large phytoplankton consists of the diatoms group in ERSEM, ECOSMO, ERGOM and PISCES, and the sum of diatoms and dinoflagellates groups in BFM. The ratio has no unit.

G) the **Phytoplankton phenology** consists of three indicators: the value of the maximum of chlorophyll concentration in the layer 0-5m (mgChl m^{-3}), the depth of the maximum of chlorophyll during the summer period (m) and the timing of the bloom, i.e. the tome of the year when the two maxima occur (day).

2.3 The observable variables

To constrain the biogeochemical indicators listed in Section 2.2, we need to identify which observable variables should be assimilated, coherently with the objective of this work. The criteria for the preliminary selection of these observable variables are that: i) they can be monitored operationally by current observational platforms, and ii) they are simulated by the current operational models.

The specific definitions of the observed variables require considering how the variables are defined in the different assimilative models of CMEMS. For example, ocean-colour chlorophyll observations match different types and numbers of phytoplankton functional types in models of different complexity. In addition, the definition of the observable variables differs in relation to the observation platform; for example, ocean-colour refers to chlorophyll up to the mixed layer depth (MLD), while biogeochemical-Argo and gliders refers to chlorophyll profiles and transects (e.g. 0-1000m). Finally, we note that some model variables are directly constrained in the CMEMS assimilation schemes. For example, the phytoplankton carbon content are updated along with chlorophyll by using the prior chlorophyll:carbon ratio in the NWS system (e.g. Skakala et al., 2018). Therefore, we took account of the characteristic of the assimilative and observational systems of CMEMS to define the observable variable in Table 2.

Table 2.2 List and definition of the observable variables in the sensitivity analysis

Observable variable	Model state variables perturbed along with the observed variable	
1 Chlorophyll ocean colour	Chlorophyll and C, N, P (, Si) Apply the same perturbation on all PFTs state variables	In MLD
2 Chlorophyll from floats and gliders	As above	0-1000 m or 0-bottom
3 POC	Small phytoplankton + small particulate detritus + heterotrophic nano flagellates + bacteria Small means < 20 micron	0-1000m or 0-bottom
4 Nitrate	Nitrate	0-1000 m or 0-bottom
5 Phosphate	Phosphate	0-1000 m or 0-bottom
6 oxygen	Oxygen	0-1000m or 0-bottom
7 pH & pCO2	Dissolved Inorganic Carbon (DIC)	0-1000m or 0-bottom

2.4 The sites and set-up of the simulations

The analyses were performed at the 5 ocean sites shown in Figure 1 and synthesized in Table 3. They cover all the regions where the biogeochemical models described in Section 2.1.3 are used by the Copernicus Marine Service MFC. The configuration of the models for these sites was described thoroughly in the Deliverable 2.2 of SEAMLESS.

Two sites were selected to run multi-model ensemble analysis in contrasting environmental conditions. These are: 1) the coastal mesotrophic site Station "L4"; and 2) the oligotrophic open ocean site "BATS". These are characterized by different trophic regimes, phytoplankton cycles, and vertical hydrodynamics as synthetized in column 2 of Table 3.

In each of the remaining sites, analyses were performed using the specific models employed in that region by the Copernicus Marine Service (see third column in Table 3). The objective of these additional analyses was to corroborate the results obtained with those same models at sites BATS and L4, where those models had been applied for the first time in this work.

The set-up of the multi-model simulations at sites L4 and BATS used common climatological values for the initial conditions of the model state variables, derived from public datasets of the two data-rich sites (see Table 4). Atmospheric reanalyses were used to force the models. Seven-year long spin-up were performed to stabilize the levels of the physical and biogeochemical variables prior the target year of the analyses. The analyses focused on two contrasting periods of the year, i.e. when water column is either fully mixed or stratified, to evaluate the impact of the physical condition on the controllability of the ecosystem indicators. Given the different environmental characteristics of BATS and L4, different three-month periods were identified for the two sites (Table 4).

During the spin-up simulations, both biogeochemical and physical variable were nudged to climatological monthly values derived from available data. During the analyses target period, only physical nudging was applied, to guarantee an unconstrained evaluation of the sensitivities of the ecosystem indicators.

The simulations were performed on the High-Performance-Computer infrastructures of CINECA using the software of the SEAMLESS prototype described extensively in Deliverables 2.1 and 2.2

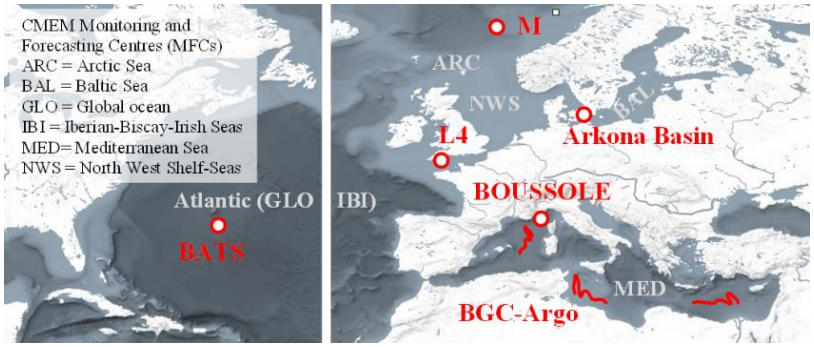

Figure 2.1 Sites (red circles) of the CMEMS Monitoring and Forecasting Centres (MFC) configured in the SEAMLESS prototype for the 1D simulations described in Table 3 below.

Table 2.3 Description of the sites where the SEAMLESS prototype was configured to perform the observability and controllability analyses.

Site location (MFC domain)	Site characteristics	Model applied (partner)	Previous 1D studies
M 66°N, 2°E (Arctic)	Spring-bloom system, open-ocean site; ~ 2000m deep	ECOSMO (NERSC)	Gharamti et al., 2017
Arkona Basin 54°53’ N13°52’E (Baltic)	Mesotrophic, near coastal site; 42 m deep; seasonally stratified	ERGOM (AWI)	Walter et al., 2006
L4 50°15’ N 4°13’ W (North-West shelf-sea)	Mesotrophic coastal site; 50 m deep; seasonally stratified	ERSEM (PML); ECOSMO (NERSC); ERGOM (AWI); BFM (OGS); PISCES (UGA)	Butenschön et al., 2016
BOUSSOLE 43°22’N, 7°54’E (Mediterranean Sea)	Meso/oligo-trophic open-ocean site; 2400 m deep	BFM (OGS)	CMEMS SE 2018-2020 Bioptimod project
BATS 31°40’N 64°10’W (Global-Atlantic)	Oligotrophic open-ocean site; 4500 m deep; general strong stratification	ERSEM (PML); ECOSMO(NERSC); ERGOM (AWI); BFM (OGS); PISCES (UGA)	Butenschön et al., 2016

Table 2.4. Set-up of the model simulations the multi-model ensemble sites

Site	BATS	L4
Initial conditions	Climatology from data of BATS station (http://bats.bios.edu/bats-data/)	Climatology from data of Western Channel Observatory (https://www.westernchannelobservatory.org.uk/)
Meteo forcings	ERA5 reanalysis of Copernicus Climate Change Service (C3S) Climate Data Store (CDS) (https://cds.climate.copernicus.eu)	ERA5 reanalysis of Copernicus Climate Change Service (C3S) Climate Data Store (CDS) (https://cds.climate.copernicus.eu)
Spin-up	5 years	7.5 years
Stratified period	15/06/2019-14/09/2019	01/06/2014-01/09/2014
Fully mixed period	01/01/2019-31/03/2019	01/11/2014-31/01/2015

3. Results part 1 – What marine ecosystem indicators can we estimate by means of data assimilation?

3.1 Introduction

This section describes the specific methods and results of Task 3.2a "Observability and controllability analysis". The aim of this subtask is to identify what ecosystem indicators can be estimated by assimilating biogeochemical variables in the CMEMS model. This objective was achieved through a sensitivity analysis of the simulated indicators with respect to the initial conditions of the observable variables.

3.2 Sensitivity analysis approach

Data assimilation analyses typically correct the values of the observed variables toward the observations of those variables, or towards functions of those observations. These analyses can impact also model variables that are not observed, e.g. target ecosystem indicators, in two different ways. The direct way is in a multivariate analysis step, where estimated covariances among variables are used to update (or "re-initialize") variables that are linked to the observed ones. The indirect way is through the simulated ecosystem processes during the integration of the model equations, i.e. in the forecast-step re-initialized in the analysis. In both ways, we expect that the re-initialization, i.e. assimilation, of an observed variable has an impact on the unobserved indicator if they are linked in the coded ecosystem processes. Here we focused on the controllability from daily to seasonal scale, which are of main interest in an operational forecast system like CMEMS and we evaluated the average impact of the re-initialization over three-month long simulation periods.

Therefore, assessing the sensitivity of a simulated ecosystem indicator with respect to the re-initialization, i.e., initial conditions, of the observed variables was adopted as pragmatic approach to the controllability analysis. Other approaches have been applied in the literature with low-complexity models (e.g., Villaverde et al., 2019), but they still appear unpractical with higher complexity models like the marine ecosystem ones used in SEAMLESS.

The sensitivities of the ecosystem indicators with respect to the observable variables were computed performing Monte-Carlo based ensemble simulations. In these simulations, the initial conditions of the observed variable were perturbed stochastically, ensemble simulations were performed, and spatial-temporal averages of the ecosystem indicators were computed.

The sensitivities are defined as follows:

$$s_{i,j} = \frac{std\,(\bar{\bar{y}}_i)}{std\,(x_j^0)}\ \frac{mean\,(x_j^0)}{mean\,(\bar{\bar{y}})} \qquad \text{eq. 1}$$

Where $s_{i,j}$ is the sensitivity of the ecosystem indicator, i.e. y_i with respect to the initial condition of the observable variable x_j^0. The double average bars ($\bar{\bar{}}$) indicate that indicator and observable variable are averaged with respect to the vertical layers of the water column over which the indicator is defined (see Section 2.2) and with respect to the time-length of the simulation period (see Table 4). "Std" and "mean" represent the standard deviation and mean value of the variable across the Monte Carlo ensemble.

The sensitivity $s_{i,j}$ normalizes the dispersion of the variables by their average values and is therefore dimensionless. The higher its value, the higher is the impact of the observed variable on the ecosystem indicator, i.e. the observability of the latter.

The set-up of the sensitivity analysis followed well-established practices (e.g., Sankar et al., 2018):

- The probability distributions of the observable variable were set as uniform, centred on the climatological value of the variable at the study sites, with threshold +/- 50% of the nominal values for all variables, but 10% for DIC which has high absolute values.
- The number of Monte-Carlo simulation was set equal to n x 1000, where n=10 is the number of ecosystem indicators.

The analysis was performed using the SEAMLESS prototype software, run on the CINECA High-Performance Computer.

3.3 Results and discussion

The results of the controllability analysis are synthetized in Figure 3.1 for both BATS (upper panel) and L4 (lower panel).

The controllability of the ecosystem indicators depends on the ocean sites to some extent since their sensitivities are different at station BATS and L4. For example, the indicators related to the plankton production (e.g., NPP, phenology, efficiency and POC) are more sensitive at BATS than at L4, with

respect to the vertical observations of nutrients and chlorophyll (ARGO_NO3, ARGO_PO4 and ARGO_CHL). This is likely related to the different trophic regimes and depths of the two sites: L4 is a mesotrophic shallow coastal site, while BATS is oligotrophic and in the open-ocean, see Figure 2.1).

The controllability of the indicators at two sites depends upon their trophic regimes. At the oligotrophic BATS, the primary production is phosphate limited in the simulations of most SEAMLESS models (not shown), and this is coherent with previous literature findings (e.g. Steinberg et al., 2001). That explains the control of phosphate observations (ARGO_PO4) upon all the ecosystem indicators simulated at BATS (upper panel in Figure 3.1), in both mixed (more evident) and stratified conditions (less evident). On the other hand, in the mesotrophic L4 (lower panel), nutrients limit production at the surface only in the summer stratified season. That explains the marked control of phosphate profiles on both the maximum and timing of the surface chlorophyll during the stratified season ("Max chl 5m" and "Max chl Timing", respectively). On the other hand, at L4, nutrient profiles do not control indicators in the winter fully mixed conditions, when nutrients concentrations are higher and plankton production is lower because light-limited.

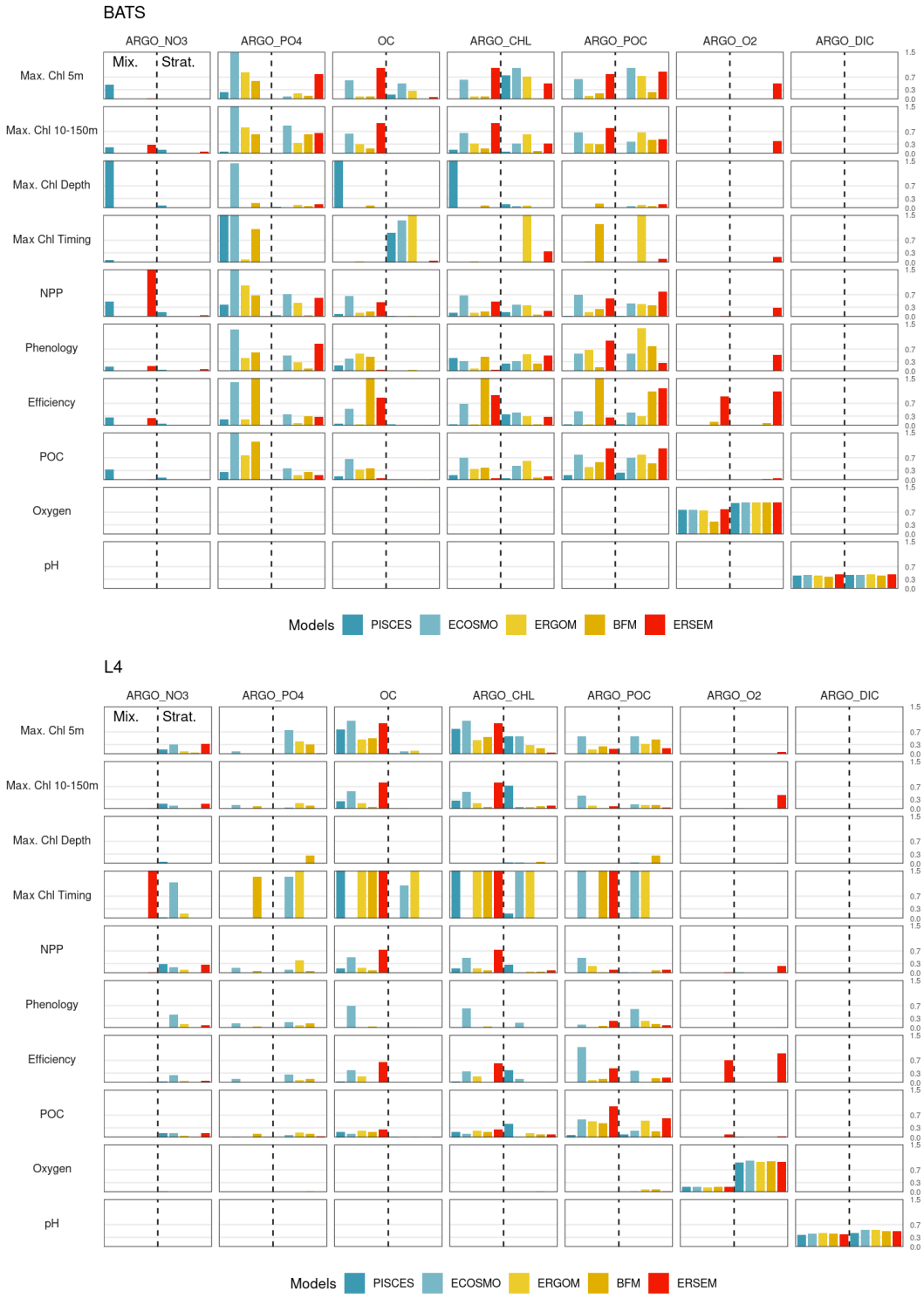

Figure 3.1. Results of the sensitivity analysis of the ecosystem indicators with respect to the observed variables at station BATS (upper panel) and L4 (lower panel). The height of the bars shows the magnitude of the sensitivities in eq.1, for the ten ecosystem indicators (rows), with respect to the seven observed variables (columns), during two representative seasons (mixed and stratified water column), computed with each of the five biogeochemical models (colours).

Plankton production and efficiency indicators are often more sensible to POC profiles than to the chlorophyll ones, at both sites and water column conditions. This is because chlorophyll is a prognostic variable in all the models (but ERGOM), and its ratio to carbon is variable as a function of the light conditions. On the other hand, the indicators NPP, trophic efficiency and PFTs are defined in carbon units, or in nitrogen units that have a constant Redfield ratio to carbon (that is the case of ERGOM, Section 2.2). That suggests that the carbon-related observations (i.e., POC) have a relative stronger control than chlorophyll observations on production indicators measured in nutrient units. In our ERGOM configuration, chlorophyll has a fixed ratio to nutrients and therefore its ocean-colour and profiles observations controls trophic efficiency as strongly as the phosphate and POC profiles.

The observability of some indicators is related to the physical state of the water column, more than to the trophic characteristics of the ocean site. This is the case of ocean colour observations, which are defined as chlorophyll in the mixed layer. When the column is stratified, ocean colour can control only the magnitude and timing of the surface chlorophyll maximum, which is defined in the upper 5 meters at both sites.

On the other hand, ocean colour can control several biogeochemical indicators when the water column is fully mixed, at both L4 and BATS. At L4, the mixed layer depth reaches the bottom of the water column when fully mixed and ocean colour can control indicators integrated from surface to the bottom 50 m deep. At BATS the simulated maximum depth of the mixed layer reaches the 200 m (not shown), and ocean colour can control the POC, NPP and the phytoplankton indicators that are integrated from the surface to that same depth (see the definitions in Section 2.2).

The features of the oxygen and pH are different from those of the other ecosystem indicators. They are sensible only to the direct measurements of oxygen itself and dissolved inorganic carbon (DIC) which forces the carbonate system. Symmetrically, oxygen and DIC observations can control the above two indicators only, for most of the models. For oxygen, these results are explained by the fact that the oxygen levels do not significantly limit the ecosystem production at the sites and depth investigated in this work. Similarly, DIC limitation is not effective at the sites, or even represented in the models, considered in this work. Therefore, it only influences the prognostic variables of the carbonate systems.

Interestingly, oxygen simulations are less controllable by the observations when the water column is mixed and gas exchanges with the atmosphere at the surface impact the concentrations in the whole water column. When the water column is stratified, the oxygen profile keeps memory of the initial conditions throughout the simulation period.

Finally, we note that the controllability of the indicators depends upon the model being used. For example, at BATS, phosphate observations have in general a stronger control on the indicators when using ECOSMO, rather than PISCES or ERSEM. These latter two models, on the other hand, have a stronger control on the indicators when constrained by nitrate profiles. Ultimately, these differences among models are linked to what nutrient is limiting the plankton production in the simulations. Such limitations are related to the model formulations rather than to the model performance, making less intuitive the controllability of indicators by different models. For example, nutrients have opposite

controllability on ECOSMO and ERSEM indicators, while both the models simulate comparable levels of nitrate and phosphate (Figure 3.2).

Controllability is not linked clearly to the complexity of the models. Models of different complexity can have similar controllability of some indicators. This is the case of PISCES and ERSEM with respect to nutrient constrain on the indicators, as mentioned above. Models of similar complexity can control in rather different measure the indicators. For example, the impact of ocean colour observations on ERSEM is closer to ECOSMO than to BFM.

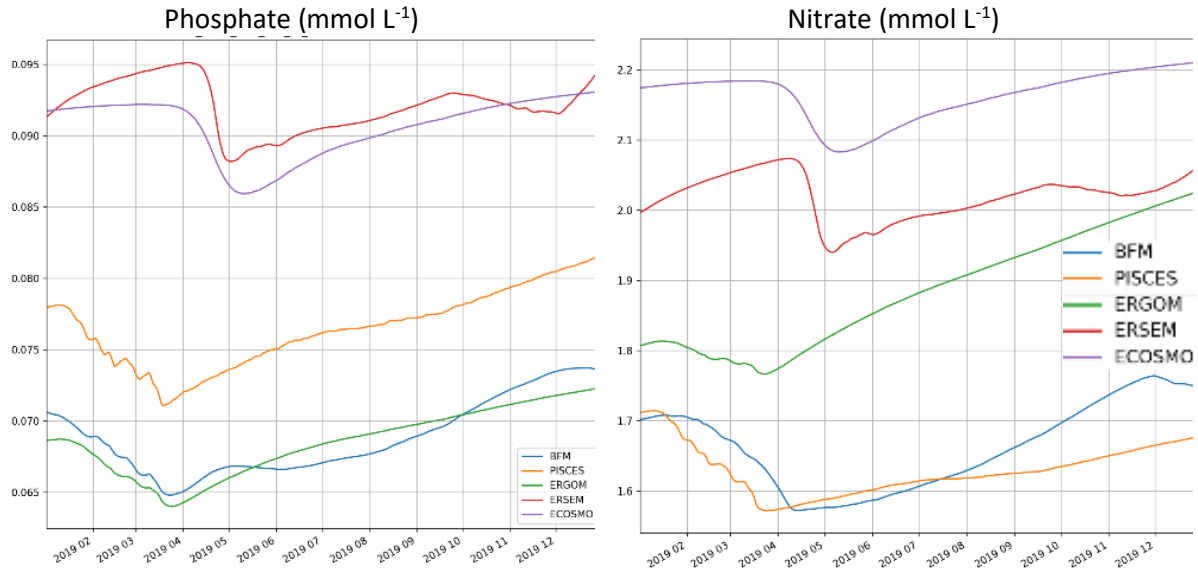

Figure 3.2 Model ensemble simulations at BATS of phosphate (left) and nitrate (right).

3.4 Concluding remarks on the results of part 1

The controllability analysis provided useful information on which, when, and where observations can be used to constrain the simulation of the SEAMLESS ecosystem indicators. However, the analyses were performed in simplified one-dimensional configurations, thus they provide a screening indication on the controllability of the indicators. Indicators that resulted controllable here, are good candidates for corroborations with the full 3-Dimensional CMEMS models. Such corroboration will be carried out in Task 3.3.

In summary, key screening results to be prioritized in the corroboration of Task 3.3 are the following:

1. ocean colour observations can control most of the ecosystem indicators in those seasons when the water column is mixed, in both coastal and ocean sites;
2. ocean colour observations can control surface indicators when the water column is stratified;
3. profiles of POC concentrations can constrain relatively well the SEAMLESS ecosystem indicators, but oxygen and pH, at both sites and physical conditions;
4. oxygen and DIC observations can constrain indicators based on oxygen concentrations and carbonate system variables.

Other results of the analysis can be translated in recommendations of "don'ts":

5. Ocean colour should not be used to control indicators below the mixed layer not only in the deep ocean, but neither in shallow but stratified coastal waters;
6. Oxygen and DIC observations cannot be used to constrain any indicator but oxygen and carbonate systems, respectively.
7. Chlorophyll is less suitable than carbon-based observations to constrain plankton production-related indicators
8. Observations of the non-limiting nutrient are less effective than the ones of the limiting nutrient in constraining the indicators, provided that the model represents correctly what the limiting nutrient is in the ecosystem.

Regarding the methodology, we evaluated the sensitivity of the indicators averaged over three-month long simulation periods. Such relatively long period is coherent with our choice to simulate the sites during periods when the water column is rather consistently mixed or stratified, increasing the likelihood that the impact of the perturbation of the initial conditions persists in time. Also, the impact might have the time to emerge in a three month period but not on shorter scales, e.g. carbon flux at depth might be registered after relatively long periods following a bloom observed by ocean-colour. However, the predictability might be shorter for some indicators in some circumstances, for example during the onset of the stratification or in highly productive periods. In such cases, the averaging period should be shorter and compatible to expected predictability of the indicator, e.g., week(s).

Finally, regarding differences among models, one should not assume that a model that fits well the observations of an indicator, is also better than a less skilled model in constraining that indicators. It is important to verify that a good model-fit is supported by a realistic representation of the ecosystem properties, rather than by compensating errors. An example is the correct representation of the correct-nutrient limitation mentioned above. Provided this verification, one can use the magnitude of the sensitivities in Figure 3.1 to assess if their specific model is suitable to constrain and indicator with selected observations. If the sensitivity is close to zero, the model is not suitable. On the other hand, setting a minimum threshold for controllability is not relevant in the one-dimensional exercise. We recommend to verify the capacity of the specific model in three-dimensional configurations, expected in the future Deliverable 3.4 " Observability of the target indicators in the 3D CMEMS MFC systems (twin experiments)".

4 Results part 2 – Sensitivity of the indicators and identifiability of the model parameters

4.1 Introduction

This section describes the specific methods and results of *Task 3.2b Parameters for ensemble generation.* The first aim of this subtask is to identify what model parameters should be perturbed to represent the uncertainty of the ecosystem indicators in ensemble assimilative simulations. This aim was pursued through a sensitivity analysis of the simulated indicators with respect to the model parameters in one-dimensional model configurations. The second aim is to assess which parameters can potentially be identified by constraining (e.g., by assimilating) the observable variables defined in Section 2.3. This aim was pursued through a sensitivity analysis of the observable variables with respect to the model parameters in one-dimensional model configurations. This approach is underpinned by the assumption that if an observable variable is sensitive to a parameter, then the opposite holds: the same parameter is "sensible" to, and can be constrained by that same observable variable.

We pursued the two above aims concurrently, by performing a joint sensitivity analysis of both the indicators and the observable variables with respect the model parameters in a Monte-Carlo based simulation framework, as described in the Methods of this section.

To investigate and compare the sensitivities of the different models, we performed the sensitivity analysis and ranked the parameters of all the models configured for the same reference stations L4 (representing a mesotrophic costal site) and BATS (representing an oligotrophic open-ocean site). In addition, to corroborate the selection of the parameters to be perturbed in the different CMEMS MFCs model domains, we performed the analysis of the one-dimensional models configured for their regional sites. The results of these two analyses are presented in two sections.

Concluding remarks drawn from the outcomes of the analysis are synthetized in a final section.

4.2 Methods of the sensitivity analysis with respect to the parameters

For each CMEMS model, a Monte Carlo sampling-based sensitivity analysis was applied to rank the importance of all their *m* parameters X = (X_1, X_2, …, X_i …, X_m). A crude Monte Carlo sampling scheme was used to generate a number *n* of realizations of the input factor vector X. These realizations were input to *n* model simulations that computed the target model output **y** = (y_1, y_2, …, y_j …, y_l) which includes the *l* spatial-temporal averages of the ecosystem indicators plus the observable variables.

The input-output relationship was represented by means of a multiple-regression model:

$$y_j = b_0 + \sum_{i=1}^{m} b_{i,j} X_i + residuals \qquad \text{eq. 4.1}$$

and the standardized regression coefficients $\beta_{i,j}$ were used as global sensitivity indices of the input factors (Saltelli et al., 2008):

$$\beta_{i,j} = \frac{b_{i,j}\sigma_{X_i}}{\sigma_{y_j}} \qquad \text{eq. 4.2}$$

Where σ_{X_i} and σ_{y_j} are the standard deviations of the realizations of the input factor X_i and of the model output y_j, respectively. The regression coefficients in Eq. (4.2) provide meaningful parameter rankings only when the linear regression explains a relatively large fraction of the model output variability (Saltelli et al., 2000).

The higher the absolute value of $\beta_{i,j}$, the higher is the rank of the associated parameter X_i with respect to the indicator or observable variably y_i.

The set-up of the sensitivity analysis followed well-established practices (e.g., Sankar et al., 2018):

- The probability distributions of the parameters were set as uniform, centred on the climatological value of the variable at the study sites, with threshold +/- 30% the nominal value.
- The number of Monte-Carlo simulation was set equal to m x 30, where m is the number of model parameters.

The sensitivity/ranking analyses of all the models were first performed at the sites L4 and BATS. For each site, the sensitivity analyses were performed in two contrasting periods, i.e., when the water column is mixed or seasonally stratified (see Section 2.4). To derive a synthetic index, the overall ranking of each parameter was computed by averaging the $\beta_{i,j}$ across indicators and observable variables, sites, and simulation periods. Such average sensitivity provides an indication of the overall impact of the parameter on the relevant model outputs, including contrasting physical conditions of the water column.

Additional analyses were performed with each CMEMS model at their regional site.

To compare the rankings of parameters in different models, we mapped the parameters into broad groups, as suggested in Sankar et al., 2018 (see Table 4.1). Such groups represent categories such as biogeochemical processes and functional groups.

The analyses were performed using the SEAMLESS prototype software, run on the CINECA High-Performance Computer.

Table 4.1 Group of parameters defining categories such as biogeochemical processes and functional groups that are common to the different models investigated in this work (modified from Sankar et al., 2018).

Group	Description
1	Photosynthetic parameters
2	Metabolic carbon lost parameters (respiration)
3	Lost carbon by lysis parameters
4	Nutrient parameters
5	Q_{10} parameters : regulating temperature factors
6	Photosynthetically available fraction of irradiation
7	Other primary production parameters
8	Maximum specific gross uptake of bacteria
9	Bacterial loss parameters
10	Nutrient uptake / remineralization
11	Additional nutrient remineralization
12	Other bacteria parameters
13	Maximum zooplankton uptake
14	Zooplankton loss parameters
15	Q_{10} of zooplankton
16	Zooplankton nutrient quotas
17	Food matrix parameters
18	Deep-water remineralization closure parameters
19	Sedimentation parameters
20	Cellular structural parameters
21	Light extinction parameters

4.3 Results and discussion

The results of the sensitivity and ranking analyses of all the models at the representative sites L4 and BATS and of each model in its regional sites are presented separately in the following.

4.3.1 Representative sites BATS and L4

The most relevant parameters of each model are listed in Table 4.2.

In **PISCES**, the constants defining the parameterization of bacterial remineralization of organic matter resulted the most relevant (groups 10-12). In fact, this intermediate complexity model does not include bacteria as a dynamic state variable. The parameters linked to the plankton growth (i.e. to the light and temperature forcings and maximum growth rate) and plankton food chain (zooplankton grazing rates and preferences) were also important.

In **ECOSMO**, the light parameter resulted the most important. Followed by plankton growth and grazing rates. The remineralization parameters are relatively less important. Interestingly, the phosphate half saturation ranked among the 10 most important parameters. This finding is coherent with the sensitivity of the ecosystem indicators to the observations of nitrate in Figure 3.1.

In **ERGOM**, plankton trophic links and sediment remineralization parameters ranked comparatively high. The relevance of light-related parameters ranked fourth, but with a comparatively low score (66%).

In both the high-complexity models, **BFM** and **ERSEM**, the light and bacteria-related parameters scored the highest ranks. These are followed by quite different plankton-related parameters in the two models: in BFM the parameters linked to the small types of plankton are more important (i.e., picophytoplankton and microzooplankton), while in ERSEM the parameters linked to the large types of plankton are more important (diatoms and nanophytoplankton). An additional interesting difference among the two models regards the ranking of the nutrient limitation parameters. In BFM phosphate-related parameters are relatively important: the minimum phosphorus to carbon ratio in picophytoplankton ranks 8. This result contrasts with the higher importance of four nitrate-related parameters in ERSEM: the maximum nitrogen to carbon ratio as well as threshold of nitrogen limitation for both diatoms and nanophytoplankton all rank among the 10 most important parameters. The differences in the nutrient-limitation parameters are coherent with the differences in the controllability of the indicators with respect to the observations of nitrate in ERSEM, rather than phosphate in BFM Figure 3.1.

The difference in the sensitivities of BFM and ERSEM are likely related to differences in their formulations targeting the North-East Atlantic (ERSEM), dominated by larger size-fractions of plankton (Ciavatta et al., 2018), and the Mediterranean Sea (BFM), which is phosphate limited and dominated by smaller size-fractions of plankton (Ciavatta et al., 2019; Alvarez et al., 2022).

Table 4.2 Rank of the parameters based on the overall sensitivities of the ecosystem indicators and observable variables simulated by the models at stations L4 and BATS. Notation and description of the parameters are reported. The score is computed by normalizing the β_j in eq. 4.2 by the highest β value of the parameter ranking first. The Group refer to the categories 1-21 in Table 4.1.

PISCES				
Rank	**Notation**	**Description**	**Score**	**Group**
1	dom_rem/xremik	DOM remineralization rate	100%	[10]
2	dom_rem/xkdoc	DOC half-saturation constant in limiting bacterial DOM degradation activity (Aumont et al, Eq 34)	99%	[12]
3	Optics/parlux	PAR : SWR ratio	93%	[6]
4	zoo/xprefn	Microzooplankton preference for nanophyto	91%	[17]
5	Dia/mumax0	Diatoms Max Growth	90%	[1]
6	Phy/logbp	Nanophyto temperature sensitivity for growth	88%	[5]
7	zoo/grazrat	MicroZoo maximum grazing rate	85%	[13]
8	phy/mumax0	Nanophyto Max Growth	83%	[1]
9	dia/logbp	Diatoms Temperature sensitivity for growth	81%	[5]
10	phy/padlopers	Nanophyto P-I slope	67%	[1]

ECOSMO				
Rank	**Notation**	**Description**	**Score**	**Group**
1	g2	E-folding depth of visible fraction (m)	100%	[6]
2	muPs	Maximum growth rate of small Phytoplankton	83%	[1]
3	mPs	Small Phytoplankton mortality rate	69%	[3]
4	A	non-visible fraction of shortwave radiation	66%	[6]
5	GrZsP	Grazing rate of small Zooplankton on Phytoplankton	64%	[13]
6	gammaZsp	Small Zooplankton assimilation efficiency on Phytoplankton	52%	[13]
7	reminD	Detritus remineralization rate	42%	[10,18]
8	alfaPs	Initial slope of P-I curve for small Phytoplankton	41%	[1]
9	rPO4	PO4 half saturation	38%	[10]
10	Rg	Half saturation rate for Zooplankton	37%	[13,16]

ERGOM				
Rank	**Notation**	**Description**	**Score**	**Group**
1	rp0	Diatoms uptake rate	100%	[17]
2	q10_rec	sediment recycling q10 rule factor	98%	[5]
3	rfr	Redfield ratio P/N	79%	[1]
4	imin_di	minimal optimal light radiation, diatoms	66%	[21]
5	graz	Zooplankton grazing rate	55%	[13]
6	deltao	Phytoplankton mortality rate (pl -> dd)	49%	[10]
7	dn	Detritus mineralization rate (dd -> aa)	45%	[17 or 11]
8	rf0	Flagellates uptake rate	44%	[12]
9	iv	Ivlev constant, quadratic	42%	[11]
10	zcl1	Zooplankton closure parameter	40%	[14]

BFM				
Rank	**Notation**	**Description**	**Score**	**Group**
1	light/EPS0r	Background shortwave attenuation	100%	[21]
2	light/pEIR_eow	Photosynthetically active fraction of shortwave radiation	57%	[6]
3	B1/p_pu_ra	Activity respiration fraction, bacteria	55%	[9]
4	Z5/p_pu	Assimilation efficiency, microzooplankton	44%	[13]
5	P3/p_q10	Q10 coefficient, picophytoplankton	40%	[5]
6	Z4/p_sds	Exponent of density-dependent mortality, omnivorous mesozooplankton	38%	[14]
7	P3/p_qlcPPY	Reference Chla:C quotum, picophytoplankton	35%	[1]
8	P3/p_qplc	Minimum phosphorus to carbon ratio, picophytoplankton	33%	[4]
9	P3/p_temp	Cut-off threshold for temperature factor, picophytoplankton	32%	[5]
10	P2/p_qlcPPY	Reference Chla:C quotum, nanophytoplankton	32%	[1]

ERSEM				
Rank	**Notation**	**Description**	**Score**	**Group**
Group				
1	light/PEIR_eow,	photosynthetically active fraction of shortwave radiation,	100%	[6]
2	B1/pu	efficiency at high oxygen levels (bacteria)	92%	[9]
3	B1/sR1	maximum turn-over rate of DOM	83%	[12]
4	light/a0w	absorption coefficient of clear water	74%	[21]
5	B1/rR2	fraction of semi-labile DOC available to bacteria	69%	[12]
6	P2/xqcn	threshold for nitrogen limitation (relative to Redfield ratio) in nanophytoplankton	61%	[20]
7	P1/xqn	maximum nitrogen to carbon ratio (relative to Redfield ratio) for diatoms	58%	[20]
8	P1/xqcn	threshold for nitrogen limitation (relative to Redfield ratio) in diatoms	57%	[20]
9	P2/xqn	maximum nitrogen to carbon ratio (relative to Redfield ratio) for nanophytoplankton	57%	[20]
10	P1/sum,	maximum specific productivity at reference temperature for diatoms,	52%	[7]

4.3.2 Regional sites

The ranking of the parameters of the five CMEMS models computed in the one-dimensional sites in their CMEMS domain is presented in Table 4.3. In general, the ranking in the specific sites corroborate the groups of parameters that resulted among the ten most significant in the reference sites L4 and BATS. In particular, for each model, the same most relevant parameter was identified in the regional and reference sites. The only exception is ERGOM, which was most sensitive to the Phytoplankton mortality rate at ARCONA, rather than the diatoms uptake rate in BATS/L4. For some models, also the ranking of the subsequent parameter was substantially unchanged, a part some shifts of position. Interestingly, sinking parameters became relevant in ECOSMO/StatM.

Thus, again, light-forcing parameters were in prominent positions in ECOSMO/StatM, BFM/Boussole and ERSEM/L4; bacteria parameterizations and parameters in PISCES/BATS, BFM/BOUSSOLE and ERSEM/L4; plankton-trophic and growth parameters in ECOSMO/StatM and ERGOM/ARCONA and, in a slightly lower positions, in PISCES/BATS, BFM/BOUSSOLE and ERSEM/L4.

Interestingly, BFM kept plankton-trophic and growth parameters among the ten most relevant in the regional as in the reference sites. However, in BFM/BOUSSOLE, the above parameters refer to the large-size fraction of the plankton community (diatoms), while in BATS/L4 they were referring to the small size (Table 4.2). BOUSSOLE is a mesotrophic site, with relevant blooms of diatoms in the winter/spring season (Deliverable 2.2). These results indicate that the parameter ranking in BFM is robust but sensitive to the trophic regime and plankton structure of the site where the analysis is performed. Also, in ERSEM/L4 the parameter related to the large-size fraction of the plankton community (diatoms and dinoflagellates), resultant relevant. But this is not dissimilar to the results obtained for the oligotrophic BATS.

Table 4.3 Rank of the parameters based on the overall sensitivities of the ecosystem indicators and observable variables simulated by the models at each regional site. Notation and description of the parameters are reported. The score is computed by normalizing the β_j in eq. 4.2 by the highest β values of the parameter ranking first. The Group refer to the categories 1-21 in Table 4.1.

PISCES/BATS				
Rank	**Notation**	**Description**	**Score**	**Group**
1	dom_rem/xremik	DOM remineralization rate	100%	[10]
2	dom_rem/xkdoc	DOC half-saturation constant in limiting bacterial DOM degradation activity (Aumont et al, Eq 34)	99%	[12]
3	zoo/xprefn	Microzooplankton preference for nanophytoplankton	93%	[17]
4	Phy/logbp	Nanophyto Temperature sensitivity for growth	86%	[5]
5	zoo/grazrat	MicroZoo maximum grazing rate	71%	[13]
6	phy/mumax0	Nanophyto Max Growth	70%	[1]
7	Zoo/resrat	MicroZoo linear mortality &	64%	[13]
8	phy/pislope_s	Nanophyto P-I slope	60%	[1]
9	zoo/logbz	Temperature sensitivity for grazing	56%	[5]
10	phy/beta1	NanoPhyto absorption in blue part of the light	56%	[21]

ECOSMO/StatM				
Rank	**Notation**	**Description**	**Score**	**Group**
1	G2	e-folding depth of visible fraction (m)	100%	[21]
2	A	non-visible fraction of shortwave radiation	83%	[6]
3	reminD	Detritus remineralization rate	77%	[10-18]
4	sinkDet	Detritus sinking rate	69%	[19]
5	muPs	Maximum growth rate of small Phytoplankton	48%	[1]
6	muPl	Maximum growth rate of large Phytoplankton	42%	[1]
7	GrZsP	Grazing rate of small Zooplankton on Phytoplankton	40%	[13]
8	GrZlP	Grazing rate of large Zooplankton on Phytoplankton	35%	[13]
9	gammaZsp	Small Zooplankton assimilation efficiency on Phytopl	34%	[13]
10	Frr	Fraction of dissolved from detritus	30%	[10-18]

ERGOM/ARCONA				
Rank	**Notation**	**Description**	**Score**	**Group**
1	deltao	Phytoplankton mortality rate (pl -> dd)	100%	[10]
2	rfr	Redfield ratio P/N	85%	[1]
3	dn_sed	Sediment mineralization rate (fl -> aa)	74%	[19]
4	iv	Ivlev constant, quadratic	74%	[11]
5	q10_rec	sediment recycling q10 rule factor	74%	[5]
6	graz	Zooplankton grazing rate	73%	[13]
7	wpz	Diatoms sinking velocity	65%	[19]
8	rp0	Diatoms uptake rate	64%	[17]
9	sfl_nn	constant surface nitrate flux	64%	[4]
10	wdz	Detritus sinking velocity	61%	[18]

BFM/BOUSSOLE				
Rank	**Notation**	**Description**	**Score**	**Group**
1	light/EPS0r	Background shortwave attenuation	100%	[21]
2	Z5/p_pu	Assimilation efficiency, microzooplankton	67%	[13]
3	light/pEIR_eow	Photosynthetically active fraction of shortwave radiation	54%	[6]
4	Z5/p_sum	Potential growth rate, microzooplankton	47%	[13]
5	P1/p_qlcPPY	Reference Chla:C quotum, diatoms	42%	[1]
6	P1/p_qup	Membrane affinity for P, diatoms	41%	[4]
7	Z5/p_pu_ea	Fraction of activity excretion, microzooplankton	36%	[14]
8	P1/p_alpha_chl	Initial slope of the P-E curve, diatoms	35%	[1]
9	P1/p_qplc	Minimum phosphorus to carbon ratio, diatoms	33%	[4]
10	P1/p_srs	Respiration rate at 10 degrees C, diatoms	33%	[2]

ERSEM/L4				
Rank	**Notation**	**Description**	**Score**	**Group**
1	light/PEIR_eow,	photosynthetically active fraction of shortwave radiation,	100%	[6]
2	B1/pu	efficiency at high oxygen levels (bacteria)	74%	[9]
3	light/a0w	absorption coefficient of clear water	71%	[21]
4	P1/sum,	maximum specific productivity at reference temperature for diatoms,	68%	[7]
5	P1/xqcn	threshold for nitrogen limitation (relative to Redfield ratio) in diatoms	64%	[20]
6	P1/xqn	maximum nitrogen to carbon ratio (relative to Redfield ratio) for diatoms	62%	[20]
7	B1/sR1	maximum turn-over rate of DOM	60%	[12]
8	B1/rR2	fraction of semi-labile DOC available to bacteria	53%	[12]
9	P1/alpha	initial slope of PI-curve (mg C m^2/mg Chl/W/d)	51%	[1]
10	P4/xqcn	threshold for nitrogen limitation (relative to Redfield ratio) in dinoflagellates	49%	[20]

4.4 Concluding remarks on the results of Part 2

The sensitivity and ranking analysis of the parameters provided useful information for each CMEMS model on: (i) which parameters should be perturbed to obtain ensemble distributions representing the uncertainty of the ecosystem indicators; (ii) which parameters has the potential to be controlled and estimated by the observable variables by means, e.g., of assimilative methods for state-parameter. This information is relevant to the delivery of the subsequent tasks of WP3 and WP6.

We noted that the analyses at the reference sites and the regional sites are coherent in identifying the most relevant parameter (rank 1) as well as the group of parameters that are within the ten most important. However, we also noted that the precise position of the parameters might change at the

reference and regional sites. We also noted some sensitivity to the regional sites, e.g., increased relevance of sinking rates and dependencies on the local trophic regime and plankton communities. Therefore, we suggest using the ranking at the regional sites (Table 4.3) if only few parameters need to be selected in computationally expensive ensemble and assimilative simulations with the full three-dimensional CMEMS models.

We also note that our Monte-Carlo based analyses were performed in simplified one-dimensional configurations, to exploit the computational efficiency of the configurations. The sensitivities might be different in three-dimensional configurations. For example, sinking parameters might have different impacts when horizontal transport is included in the simulation.

Therefore, the ranking of the parameters provided in this work should be considered as a screening analysis. This provided a sub-set of parameters which will be tested further in the three-dimensional simulations.

5 Notes on the sensitivity analysis approach

In sections 3.4 and 4.4 we remarked the significance and the exploitability of the results we have obtained in Task 3.2 of SEAMLESS. We have also pointed out some implications of the methods on the specific results presented in two sections. Here we stress the most relevant implications of the sensitivity analyses methods that are common to the two sections.

First, all the sensitivity experiments of Task 3.2 were performed in a 1-dimensional vertical modelling framework. This is indeed a useful approach when it is necessary to perform simulations of very large ensembles, such as tens of thousands in our application with biogeochemical models with more than 500 parameters. However, these 1D experiments are based on the approximation of horizontal homogeneity, e.g., negligible lateral transport and horizontal gradients. We mitigated this approximation by nudging the simulated physical variables to observed profiles, thus indirectly embedding effects that were not simulated. Nevertheless, we highlight that the conclusions obtained in Task 3.2 are only valid under the approximated one-dimensional representation of the ecosystem. In principle, indicators that are found poorly controllable in 1D, could become controllable in a 3D experimental framework exploiting information in observed horizontal patterns. Importantly, indicators that were found controllable, or parameters that were found sensitive in 1D, are good candidates to become the focus the analysis of 3D models. Task 3.3 of SEAMLESS will deal with assessing the controllability and sensitivities in the 3D configurations of the CMEMS models.

Second, the sensitivity analyses took account of only few features of the assimilation approaches used in CMEMS. For example, the preservation of the phytoplankton internal nutrient ratios in the NWS and MED analysis systems, or the spreading of the ocean-colour observations throughout the mixed layer in most of the MFC. However, the analyses did not take account of some peculiarities of the assimilation algorithms used in the CMEMS systems. For example, the controllability of dynamical systems depends on the properties of the feedback loop operators of the assimilation systems, e.g., the Kalman gain matrix or the balancing equations in variational approaches. This feedback might

become relevant also for the identifiability of the parameters, when the assimilative systems is applied to state-parameter estimation, like in the CMEMS ARC MFC. The controllability analysis in Task 3.3 will refer more specifically to the assimilative systems used in the different MFCs.

Finally, we assumed that the probability distributions of the observable variables and of the parameters were uniform in the sensitivity analyses. We note that this approach is rather common in the literature with marine models (e.g., Sankar et al., 2018) and was adopted here as well for the sake of simplicity. However, we note that more refined approaches have been adopted in the literature (e.g., Prieur et al., 2019).

6 References

Álvarez, E., Lazzari, P. and Cossarini, G., 2022. Phytoplankton diversity emerging from chromatic adaptation and competition for light. *Progress in Oceanography*, 204, p.102789.

Armengol, L., Calbet, A., Franchy, G., Rodríguez-Santos, A. and Hernández-León, S., 2019. Planktonic food web structure and trophic transfer efficiency along a productivity gradient in the tropical and subtropical Atlantic Ocean. *Scientific reports*, *9*(1), pp.1-19.

Artioli, Y., Blackford, J.C., Butenschön, M., Holt, J.T., Wakelin, S.L., Thomas, H., Borges, A.V. and Allen, J.I., 2012. The carbonate system in the North Sea: Sensitivity and model validation. *Journal of Marine Systems*, *102*, pp.1-13.

Aumont, O., Éthé, C., Tagliabue, A., Bopp, L. and Gehlen, M., 2015. PISCES-v2: an ocean biogeochemical model for carbon and ecosystem studies. *Geoscientific Model Development*, *8*(8), pp.2465-2513.

Bagniewski, W., Fennel, K., Perry, M.J. and D'asaro, E.A., 2011. Optimizing models of the North Atlantic spring bloom using physical, chemical and bio-optical observations from a Lagrangian float. *Biogeosciences*, *8*(5), pp.1291-1307.

Baretta-Bekker, J.G., Baretta, J.W. and Rasmussen, E.K., 1995. The microbial food web in the European regional seas ecosystem model. *Netherlands Journal of Sea Research*, *33*(3-4), pp.363-379.

Bopp, L., Lévy, M., Resplandy, L. and Sallée, J.B., 2015. Pathways of anthropogenic carbon subduction in the global ocean. *Geophysical Research Letters*, *42*(15), pp.6416-6423.

Brasseur, P., Gruber, N., Barciela, R., Brander, K., Doron, M., Elmoussaoui, A., Hobday, A.J., Huret, M., Kremeur, A.S., Lehodey, P. and Matear, R., 2009. Integrating biogeochemistry and ecology into ocean data assimilation systems. *Oceanography*, *22*(3), pp.206-215.

Butenschön, M., Clark, J., Aldridge, J.N., Allen, J.I., Artioli, Y., Blackford, J., Bruggeman, J., Cazenave, P., Ciavatta, S., Kay, S. and Lessin, G., 2016. ERSEM 15.06: a generic model for marine biogeochemistry and the ecosystem dynamics of the lower trophic levels. *Geoscientific Model Development*, *9*(4), pp.1293-1339.

Canu, D.M., Ghermandi, A., Nunes, P.A., Lazzari, P., Cossarini, G. and Solidoro, C., 2015. Estimating the value of carbon sequestration ecosystem services in the Mediterranean Sea: An ecological economics approach. *Global Environmental Change*, *32*, pp.87-95.

Ciavatta, S., Brewin, R.J.W., Skakala, J., Polimene, L., de Mora, L., Artioli, Y. and Allen, J.I., 2018. Assimilation of ocean-color plankton functional types to improve marine ecosystem simulations. *Journal of Geophysical Research: Oceans*, *123*(2), pp.834-854.

Ciavatta, S., Kay, S., Brewin, R.J., Cox, R., Di Cicco, A., Nencioli, F., Polimene, L., Sammartino, M., Santoleri, R., Skakala, J. and Tsapakis, M., 2019. Ecoregions in the Mediterranean Sea through the reanalysis of phytoplankton functional types and carbon fluxes. *Journal of Geophysical Research: Oceans*, *124*(10), pp.6737-6759.

Cossarini, G., Lazzari, P. and Solidoro, C., 2015. Spatiotemporal variability of alkalinity in the Mediterranean Sea. *Biogeosciences*, *12*(6), pp.1647-1658.

Cushing, D.H., 1989. A difference in structure between ecosystems in strongly stratified waters and in those that are only weakly stratified. *Journal of plankton research*, *11*(1), pp.1-13.

Daewel, U. and Schrum, C., 2013. Simulating long-term dynamics of the coupled North Sea and Baltic Sea ecosystem with ECOSMO II: Model description and validation. *Journal of Marine Systems*, *119*, pp.30-49.

Eddy, T.D., Bernhardt, J.R., Blanchard, J.L., Cheung, W.W., Colléter, M., Du Pontavice, H., Fulton, E.A., Gascuel, D., Kearney, K.A., Petrik, C.M. and Roy, T., 2021. Energy flow through marine ecosystems: confronting transfer efficiency. *Trends in Ecology & Evolution*, *36*(1), pp.76-86.

Garnier, F., Brankart, J.-M., Brasseur, P., & Cosme, E. (2016). Stochastic parameterizations of biogeochemical uncertainties in a 1/4° NEMO/PISCES model for probabilistic comparisons with ocean color data. Journal of Marine Systems, 155, 59–72.

Gharamti, M.E., Tjiputra, J., Bethke, I., Samuelsen, A., Skjelvan, I., Bentsen, M. and Bertino, L., 2017. Ensemble data assimilation for ocean biogeochemical state and parameter estimation at different sites. *Ocean Modelling*, *112*, pp.65-89.

Geider, R.J., MacIntyre, H.L. and Kana, T.M., 1997. Dynamic model of phytoplankton growth and acclimation: responses of the balanced growth rate and the chlorophyll a: carbon ratio to light, nutrient-limitation and temperature. *Marine Ecology Progress Series*, *148*, pp.187-200.

Goodliff, M., Bruening, T., Schwichtenberg, F., Li, X., Lindenthal, A., Lorkowski, I., Nerger, L., 2019. Temperature assimilation into a coastal ocean-biogeochemical model: Assessment of weakly and strongly-coupled data assimilation, Oce. Dyn., 69, 1217-1237

Lazzari, P., Solidoro, C., Salon, S. and Bolzon, G., 2016. Spatial variability of phosphate and nitrate in the Mediterranean Sea: A modeling approach. *Deep Sea Research Part I: Oceanographic Research Papers*, *108*, pp.39-52.

Lazzari, P., Solidoro, C., Salon, S. and Bolzon, G., 2016. Spatial variability of phosphate and nitrate in the Mediterranean Sea: A modeling approach. *Deep Sea Research Part I: Oceanographic Research Papers*, *108*, pp.39-52.

Lefort, S., Aumont, O., Bopp, L., Arsouze, T., Gehlen, M. and Maury, O., 2015. Spatial and body-size dependent response of marine pelagic communities to projected global climate change. *Global change biology*, *21*(1), pp.154-164.

Legendre, L. and Rassoulzadegan, F., 1995. Plankton and nutrient dynamics in marine waters. *Ophelia*, *41*(1), pp.153-172.

Lessin, G., Raudsepp, U., Stips, A., 2014. Modelling the influence of major Baltic inflows on near-bottom conditions at the entrance of the Gulf of Finland. *PLOS ONE*, 9, e112881

Maar, M., Møller, E.F., Larsen, J., Madsen, K.S., Wan, Z., She, J., Jonasson, L. and Neumann, T., 2011. Ecosystem modelling across a salinity gradient from the North Sea to the Baltic Sea. Ecological Modelling, 222, 1696–1711.

Neumann, T., 2000 Towards a 3D-ecosystem model of the Baltic Sea. Journal of Marine Systems, 25, 405–419.

Prieur, C., Viry, L., Blayo, E. and Brankart, J.M., 2019. A global sensitivity analysis approach for marine biogeochemical modeling. Ocean Modelling, 139, p.101402.

Salon, S., Cossarini, G., Bolzon, G., Feudale, L., Lazzari, P., Teruzzi, A., Solidoro, C. and Crise, A., 2019. Novel metrics based on Biogeochemical Argo data to improve the model uncertainty evaluation of the CMEMS Mediterranean marine ecosystem forecasts. *Ocean Science*, *15*(4), pp.997-1022.

Saltelli, A., Chan, K., & Scott, M. (2000). Handbook of sensitivity analysis. Probability and Statistics Series.

Sankar, S., Polimene, L., Marin, L., Menon, N.N., Samuelsen, A., Pastres, R. and Ciavatta, S., 2018. Sensitivity of the simulated Oxygen Minimum Zone to biogeochemical processes at an oligotrophic site in the Arabian Sea. Ecological Modelling, 372, pp.12-23.

Skákala, J., Ford, D., Brewin, R.J., McEwan, R., Kay, S., Taylor, B., de Mora, L. and Ciavatta, S., 2018. The assimilation of phytoplankton functional types for operational forecasting in the northwest European shelf. *Journal of Geophysical Research: Oceans*, *123*(8), pp.5230-5247.

Skakala, J., Bruggeman, J., Brewin, R.J., Ford, D.A. and Ciavatta, S., 2020. Improved representation of underwater light field and its impact on ecosystem dynamics: A study in the North Sea. *Journal of Geophysical Research: Oceans*, *125*(7), p.e2020JC016122.

Sotillo, M.G., Cailleau, S., Lorente, P., Levier, B., Aznar, R., Reffray, G., Amo-Baladrón, A., Chanut, J., Benkiran, M. and Alvarez-Fanjul, E., 2015. The MyOcean IBI Ocean Forecast and Reanalysis Systems: operational products and roadmap to the future Copernicus Service. *Journal of Operational Oceanography*, *8*(1), pp.63-79.

Steinberg, D.K., Carlson, C.A., Bates, N.R., Johnson, R.J., Michaels, A.F., Knap, A.H., 2001. Overview of the US JGOFS Bermuda Atlantic Time-series Study (BATS): a decade-scale look at ocean biology and biogeochemistry. Deep Sea Res. Part II Top. Stud. Oceanogr. 48, 1405–1447. https://doi.org/10.1016/S0967-0645(00)00148-X

Vichi, M., Pinardi, N. and Masina, S., 2007. A generalized model of pelagic biogeochemistry for the global ocean ecosystem. Part I: Theory. *Journal of Marine Systems*, *64*(1-4), pp.89-109.

Vichi, M., Lovato, T., Mlot, E.G. and McKiver, W., 2015. Coupling BFM with ocean models. *Nucleus for the European Modelling of the Ocean, Release*, *1*.

Villaverde, "Observability and Structural Identifiability of Nonlinear Biological Systems", Complexity, vol. 2019, Article ID 8497093, 12 pages, 2019. doi.org/10.1155/2019/8497093

Walter, S., Breitenbach, U., Bange, H.W., Nausch, G. and Wallace, D.W., 2006. Distribution of N 2 O in the Baltic Sea during transition from anoxic to oxic conditions. *Biogeosciences*, *3*(4), pp.557-570.